This paper describes objective technical results and analysis. Any subjective views or opinions that might be expressed in the paper do not necessarily represent the views of the U.S. Department of Energy or the United States Government.

WILEY-VCH
SAND2020-0090J

GaN/InGaN blue LEDs on polycrystalline molybdenum metal foils by ion beam assisted deposition

Abdelrahman Tarief Elshafiey[1], Kenneth M. DaVico[1], Ashwin K. Rishinaramangalam[1], Arman Rashidi[1], Andrew Aragon[1], Daniel Feezell[1], Brendan P. Gunning[2], Christopher Sheehan[3], and Vladimir Matias[3]*

[1]Center for High-Technology Materials, the University of New Mexico, Albuquerque, NM 87106, USA
[2]Sandia National Laboratories, Albuquerque, NM 87123, USA
[3]iBeam Materials, Santa Fe, NM 87507, USA
* Email: atarief@unm.edu

Keywords: (III-Nitrides, GaN, InGaN, LEDs, metal foils)

We demonstrate LED arrays fabricated on a polycrystalline metal substrate using a novel technique which enables the growth of epitaxial metal-organic chemical vapor deposition (MOCVD) GaN layers on non-single crystal substrates. Epitaxial GaN is deposited directly on metal foil by use of an intermediate ion-beam assisted deposition (IBAD) aligned layer. For a single 170-µm-diameter LED on the metal foil, electroluminescence (EL) spectrum shows a peak wavelength of ~ 452 nm and a full width at half maximum (FWHM) of ~ 24 nm. The current-voltage (I-V) characteristics show a turn-on voltage of 3.7 V, a series resistance of 10 Ω. LEDs on metal show a relative EQE that is roughly 3X lower than that of similar LEDs fabricated on a sapphire substrate. InGaN LEDs on large-area non-single-crystal substrates such as metal foils can enable large-area manufacturing, reducing production cost, and opening the door for new applications in lighting and displays.

1. Introduction

III-nitride semiconductors are widely used in many applications, including light-emitting diodes (LEDs),[1] semiconductor power devices, and RF components.[2] III-nitride devices are predominantly grown epitaxially on sapphire, free standing GaN, silicon, and silicon-carbide (SiC)

Sandia National Laboratories is a multimission laboratory managed and operated by National Technology & Engineering Solutions of Sandia, LLC, a wholly owned subsidiary of Honeywell International Inc., for the U.S. Department of Energy's National Nuclear Security Administration under contract DE-NA0003525.

substrates. However, these conventional, single crystal substrates are expensive, rigid, and of limited size, making them unsuitable for many applications that require large area, mass production, and inexpensive large-area solutions. There are a number of reports on growth and fabrication of III-nitride devices on non-single-crystal substrates.[3–6] Flexible Metal substrates can be utilized for large-area roll-to-roll manufacturing, reducing production cost and opening the door to new applications in displays, wearables and solid state lighting. The metal substrate may also provide reflection and better integration of a reflector into the structure. There are several approaches used to fabricate III-nitride devices on non-single-crystal substrates. One method is to transfer the epitaxy from one substrate to another.[7] Another method is to transfer a template for epitaxy such as a layer of graphene.[4] These techniques require extra mechanical steps that complicate the fabrication process and are not suitable for large-area manufacturing. The ultimate approach is to grow III-N layers directly on the non-single crystal substrates. The advantage of that approach is that it is then easily scalable to large areas as it does not rely on transfer techniques. One report shows the direct growth of AlGaN nanowires on flexible Ti and Ta foils by molecular beam epitaxy (MBE).[3] The authors fabricated UV nanowire LEDs on Ta that showed EL intensity 16x lower compared to similar devices on a silicon substrate. Another similar study showed the direct growth of GaN nanowires on a flexible Ti foil using plasma-assisted molecular beam epitaxy (PA-MBE).[8] The direct growth of III-nitride epitaxial layers on polycrystalline metal substrates is challenging due to the formation of crystal defects, limiting the internal quantum efficiency of LEDs. Most fabricated devices on metal substrates are based on nanowire structures to reduce the defect density in the active region compared to planar structures.[9,10] However, III-nitride nanowires have their own set of challenges such as growth optimization, fabrication process, packaging, and incompatibility with current LED technologies, which are based on planar structures.[11,12] A recent study shows a direct growth of planar red, green, and blue GaN/InGaN

LEDs on flexible Hf foils using pulsed sputtering deposition (PSD) by annealing the metal to obtain a textured substrate.[5] Metal organic chemical vapor deposition (MOCVD) methods are preferred over MBE and other PVD methods to grow III-nitride epitaxial layers on metal substrates due to the widespread use of MOCVD in the LED industry and the high-quality of MOCVD-grown materials. To the best of our knowledge, thus far there are no reports on growth of III-nitride epitaxial layers on metal substrates using MOCVD. In this paper, a novel method for growing epitaxial GaN on metal polycrystalline substrates by MOCVD is used, and we report on the first GaN/InGaN LED arrays fabricated directly on metal foils. We are making arrays of LEDs to demonstrate a prototype of a light emitting strip which could be used as a large-area lighting source.

2. Epitaxial Growth of GaN on metal

iBeam Materials has developed a process for depositing epitaxial GaN films and devices directly on unaligned substrates. This process includes an IBAD texturing process for biaxially aligning films as a template for epitaxy.[13] The IBAD process enables low-cost, large-area non-single-crystal substrates to be used as potential alternatives to single-crystal sapphire and silicon

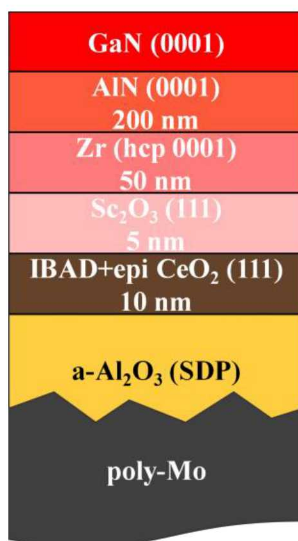

Figure 1. Schematic of the template layer structure used in the devices measured in this work. An unpolished metal substrate is used which is planarized using chemical solution deposition of amorphous alumina. This is followed by the IBAD process.

wafers for GaN electronic and optoelectronic devices. In this work, epitaxial GaN films were grown by MOCVD on these engineered templates on metal foils.

The IBAD template, as shown in **Figure 1**, consists of a metal substrate, in this case a molybdenum alloy (TZM) foil, a planarizing layer which is alumina, and the IBAD layer with further epitaxial buffer layers. We use commercial, as rolled, 60 μm thick TZM foil with a roughness of >50 nm RMS on a 5 x 5 μm scale.[14] The substrate is planarized by use of a method known as solution deposition planarization (SDP) of amorphous aluminum oxide.[14] The process is chemical solution deposition by dip coating. The end result is an alumina coated molybdenum alloy with surface roughness of less than 1 nm RMS (5x5 μm scan).[14]

10 nm of IBAD-CeO_2 with an <111> out-of-plane orientation is deposited, followed by a homoepitaxial layer and other intermediate layers to transition the lattice matching and finalized with an AlN layer of about 200 nm thickness.[13] These layers, shown schematically in Figure 1, which are in total about 300 nm thick are deposited by physical vapor deposition (reactive evaporation and reactive pulsed dc sputtering). The biaxially aligned AlN layer is then used as a template for growth of epi-GaN by MOCVD. Such GaN films of several microns have been achieved on polycrystalline molybdenum alloy foils that have typical threading dislocation densities (TDD) in GaN from plan-view TEM of 4 ~ 8 $x10^{8}$ cm^{-2}.[reference to be published] Based on the TDD in our early development of GaN-on-metal we believe that one should be able to achieve TDDs similar to those for GaN on sapphire with more development. The MOCVD growth was performed in a Veeco D125 short-jar rotating-disk reactor. Since the metal samples are flexible, the sample is either placed loosely on the platen, or, for longer pieces of tape, the sample is clamped down on the platen at the edges of the metal tape with a specially made cover plate. GaN growth was initiated at growth temperature ~1000°C on the foil substrate with no additional nucleation

layer. The base epitaxial structure consisted of 3 μm of unintentionally doped GaN and 2 μm of Si-doped *n*-GaN (doping conc. ~5x10^{18} cm^{-3}) grown at 500 Torr at temperatures of 1000-1050°C. Next, a 180 nm thick $In_{0.03}Ga_{0.97}N$ underlayer (doping conc. ~1x10^{18} cm^{-3}), a 5-period InGaN/GaN multiple-quantum well (MQW) active region consisting of 3 nm InGaN wells and 8 nm GaN barriers, a 200 nm Mg-doped *p*-GaN layer (doping conc. ~3x10^{19} cm^{-3}), and a 20 nm Mg-doped *p*+GaN contact layer (doping conc. ~1x10^{20} cm^{-3}) were grown at 300 Torr at temperatures of 830°C, 770°C, 980°C, and 900°C, respectively. A similar epitaxial structure has been grown on sapphire, with 2 μm of unintentionally doped GaN and 500 nm of Si-doped *n*+GaN (doping conc. ~1x10^{19} cm^{-3}). Next, a 40 nm thick $In_{0.025}Ga_{0.975}N$ underlayer, a 3-period InGaN/GaN multiple-quantum well (MQW) active region consisting of 3 nm InGaN wells and 6 nm GaN barriers, a 160 nm Mg-doped *p*-GaN layer (doping conc. ~2x10^{19} cm^{-3}), and a 20 nm Mg-doped *p*+GaN contact layer (doping conc. ~1x10^{20} cm^{-3}).

It is important to note that the temperatures listed above are all nominal, taken from conditions used for similar LED structures grown on sapphire wafers in the same reactor. However, the metal foils are flexible and not perfectly flat as mentioned, which results in poor thermal contact with the underlying susceptor, particularly at elevated temperatures. The foil substrates also have

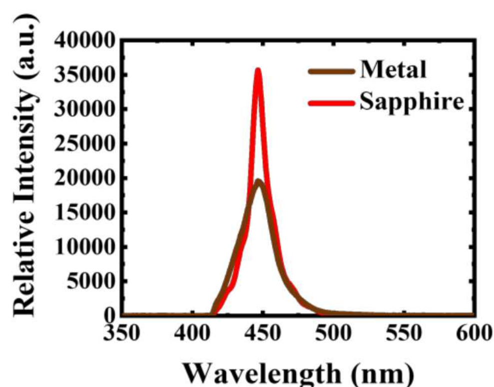

Figure 2. Relative photoluminisence (PL) measurements for QW structures grown on metal and sapphire samples

different emissivity compared to standard sapphire wafers, and in situ reflectance monitoring was not easily achievable. These observations together meant that the growth temperature required re-optimization for growth on foils. Without emissivity-corrected pyrometry, the exact measure of the foil substrate temperature is very challenging. However, based on the strong temperature sensitivity of InGaN MQWs and temperature-induced morphology changes during thick GaN growth, we found that the temperature setpoints required for the equivalent growth on IBAD substrates were about 40-80°C higher than those on sapphire (~40°C higher at ~770°C and ~80°C higher at ~1000°C). Photoluminescence (PL) measurements for the quantum well structures on metal showed typically about 55% of the signal compared to similar structures grown on sapphire (**Figure 2**).

XRD 2θ-ω scans were performed for full LED structures on both metal and sapphire as shown in **figure 3**, to verify the quality of the epilayers after growth. The FWHM of the GaN peak for both sapphire and metal samples are 0.013° and 0.020°, respectively. With the FWHM of GaN on metal being almost as twice as that on sapphire, it would be normal to expect that the dislocation density is higher on the metal sample. The TDD on sapphire is ~$2.25x10^{8}$ cm^{-2} compared to ~$5.78x10^{8}$ cm^{-2} on metal, in other words metal TDD is ~2.5X higher than sapphire TDD. However, from the 2θ-ω scan, the FWHM of GaN on the metal substrate has contributions from sample

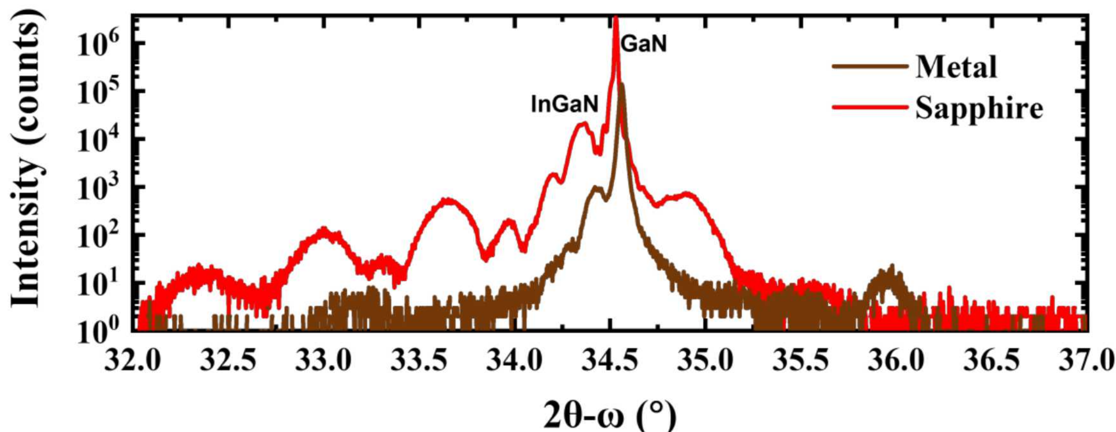

Figure 3. XRD 2θ-ω scan for full LED structures on metal and sapphire samples

curvature as well as underlying substrate roughness in addition to the dislocation density. The InGaN peaks are also observed on both metal and sapphire at roughly the same angle.

3. Fabrication of LED arrays

Figure 4(a) shows the LED fabrication process, starting with a blanket deposition of a 5/5 nm Ni/Au semi-transparent current spreading layer on the as-grown sample using electron-beam evaporation to form the *p*-contact. Then 5-µm-deep trenches were etched using an inductively coupled plasma (ICP) system to completely isolate devices and prevent shorting when devices are connected in series. Both the Ni/Au layer and the semiconductor layers were etched under the same conditions using Cl_2 plasma, with an etch rate of 100 nm/min. Next, LED circular mesas with a diameter of 170 µm were etched using ICP to reach the *n*-GaN layer, followed by depositing a 200 nm SiO_2 dielectric layer using sputter deposition system for passivating the mesa sidewalls. The dielectric layer is also used to avoid a current leakage between *n*-GaN and *p*-GaN of each device. Finally, Ti/Al/Ni/Au (20/100/50/300) and Cr/Au (30/700 nm) were deposited as the *n*-metal and *p*-metal contacts, respectively. LED arrays were fabricated on both metal and sapphire samples for

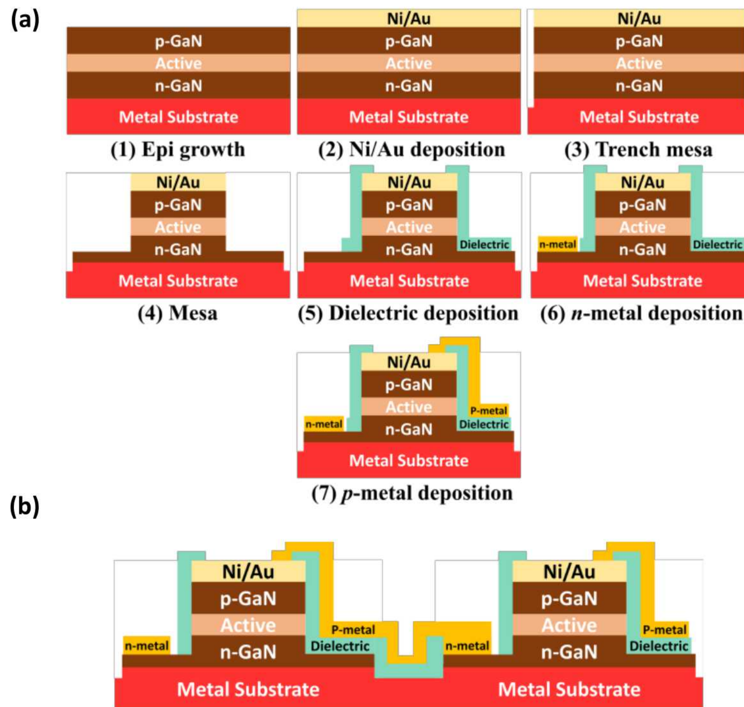

Figure 4. (a) Processing steps for the fabrication of LED arrays (b) Schematic cross section of two LED devices

comparison. Figure 4(b) shows the schematic of two LEDs connected in series. **Figure 5(a)** shows the optical microscope image of an array of LEDs fabricated on metal substrates with rows of series connected LEDs connected in parallel at the bus bars. Figure 5(b) shows a demonstration of 5 LEDs operating in series.

4. Measurements and Discussion

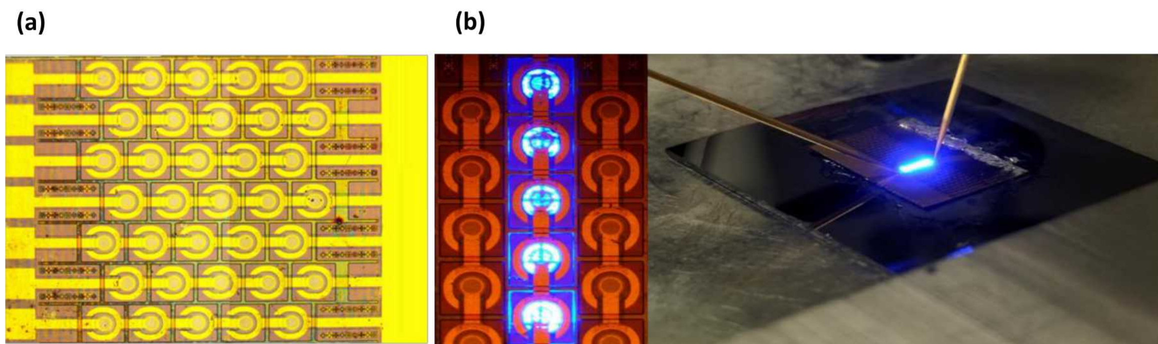

Figure 5. (a) Fabricated LED arrays on a metal sample (b) Microscope image of five LEDs in series on the metal substrate, and a photograph of the LEDs on metal bonded to a silicon wafer

Figure 6(a) and Figure 6(b) show light-current-voltage (L-I-V) characteristics and the EL spectra of different LED series containing one to five devices, respectively. A single LED device shows a peak wavelength of 452 nm, with a FWHM of 24 nm, a turn-on voltage of 3.7 V, and a series resistance of 10 ohms. I-V curves for LEDs on both metal and sapphire are depicted in Figure 6(c), where LEDs on sapphire show slightly better characteristics in the forward region. The inset of Figure 6(c) shows semi-log I-V, where the LED on metal shows a reverse leakage current of 0.4 mA compared to 0.2 μA for the LED on sapphire at -6 V. **Figure 7(a)** and figure 7(b) show the EL spectra for a single LED on metal and one on sapphire as a function of injection current,

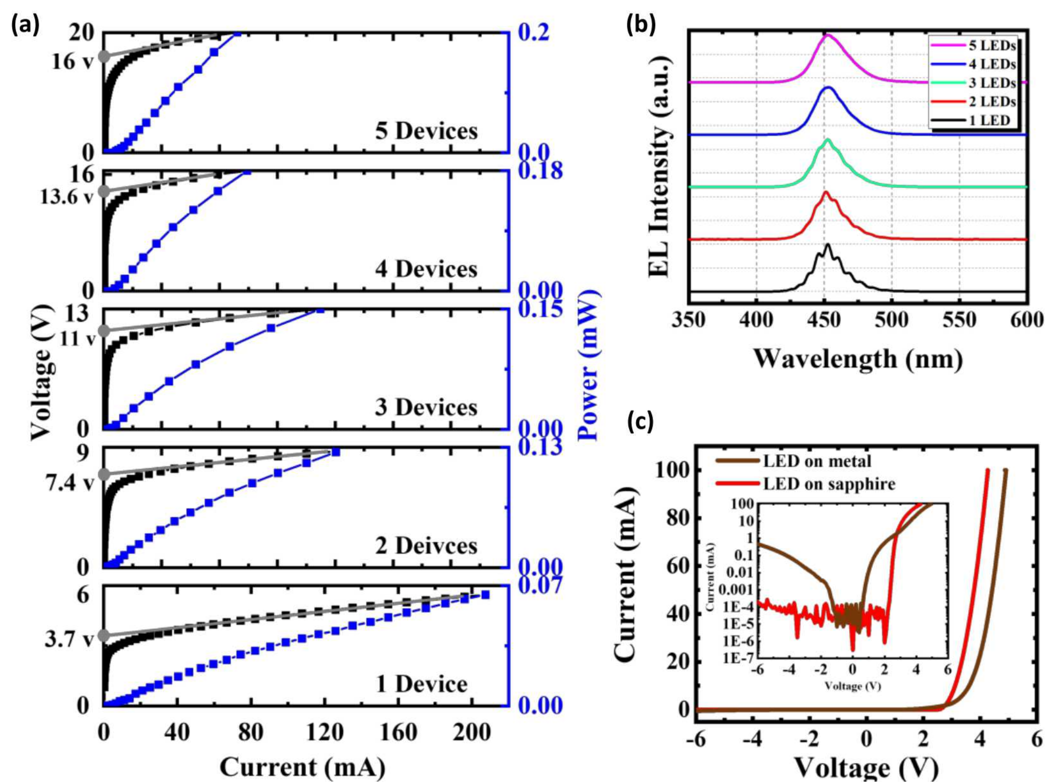

Figure 6. (a) L-I-V curves for one to five devices in series for LEDs on metal sample (b) Spectrum of one to five devices in series for LEDs on metal sample (c) I-V characteristics of an LEDs on metal vs. sapphire. The inset shows the I-V characteristics of same LEDs in semi-log scale

respectively. Peak wavelength and FWHM as a function of current and current densities are shown in figure 7(c) and figure 7(d) respectively. The peak wavelength displays a similar blue shift for both LEDs at lower current densities, confirming the presence of the quantum confined stark effect (QCSE) in the QWs of the LEDs on the metal foil. At higher current densities both LEDs show a similar red shift trend caused by bandgap shrinkage as a result of internal heating. The peak

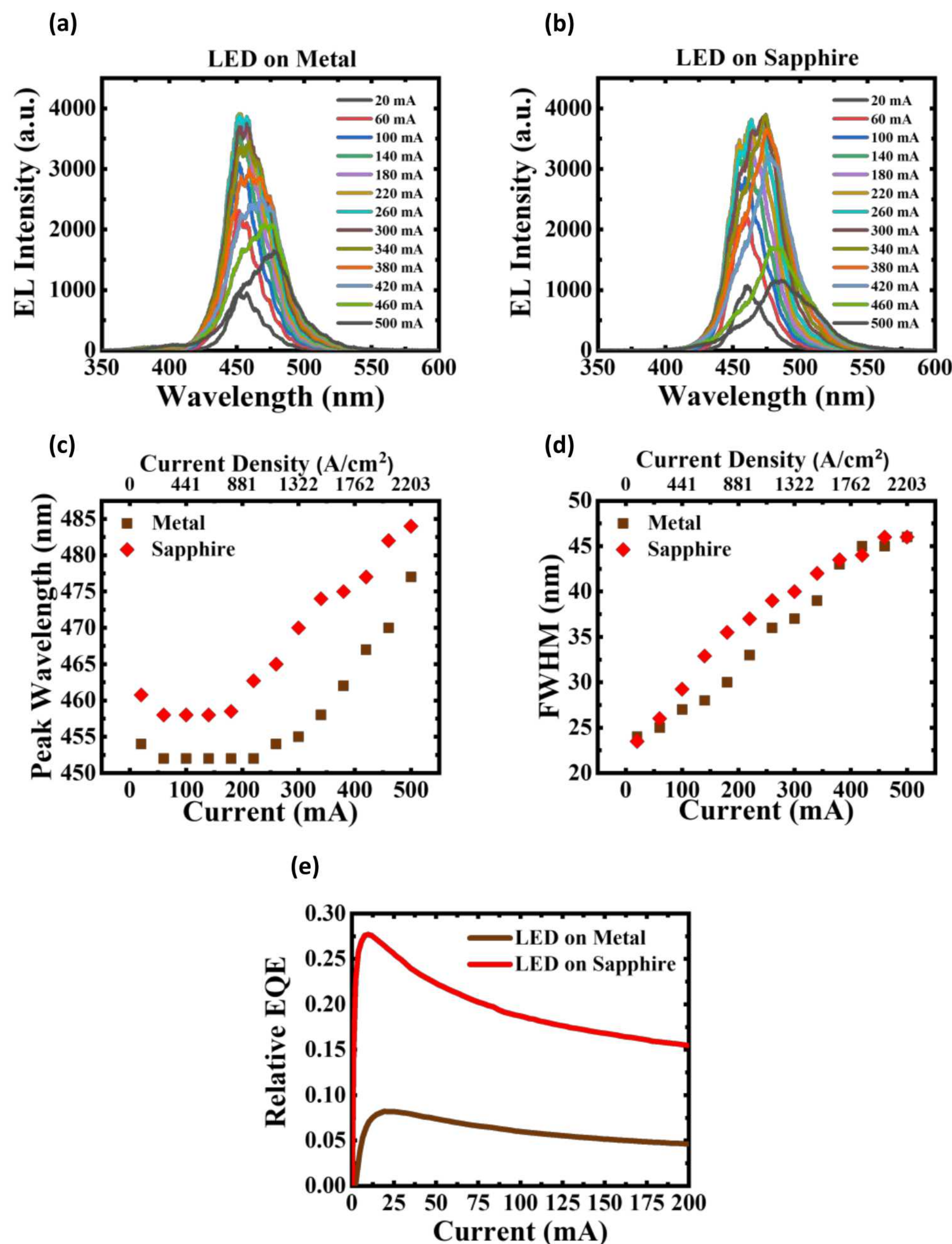

Figure 7. (a) EL spectrum vs. current for a single LED on metal (b) EL spectrum vs. current for a single LED on sapphire (c) Peak wavelength vs. current for a single LED on sapphire and metal samples (d) FWHM vs. current for a single LED on metal and sapphire samples (e) Relative EQE for single LEDs on metal and sapphire samples

wavelength of LEDs on metal is lower by ~6 nm than LEDs on sapphire, since these two samples were grown in two different reactors at different growth conditions (temperature, pressure, etc.), and the indium composition is not guaranteed to be the same. LEDs on metal show a similar FWHM to LEDs on sapphire. The relative external quantum efficiency (EQE) for single LEDs on metal and sapphire are shown in Figure 7(e). The relative EQE of the LED on metal reaches 30% of the relative EQE of the LED on sapphire. The relative EQE measurements were performed by collecting light from a single-side of the wafer into a photodetector, by keeping the photodetector and the testing probes in the same position when swapping between metal and sapphire samples. This method ensures the photodetector to be at the same angle and height for both LED devices, making the relative EQE consistent for both samples. We attribute the lower performance of the metal LEDs to the larger leakage current observed in these devices, since EQE depends on injection efficiency, which is impacted by leakage current. The leakage likely results from macroscopic defects, such as pits, that are observable in epitaxial GaN on metal (**Figure 8**). Optimization of the epitaxial layers is expected to reduce leakage current and improve EQE.

5. Conclusions

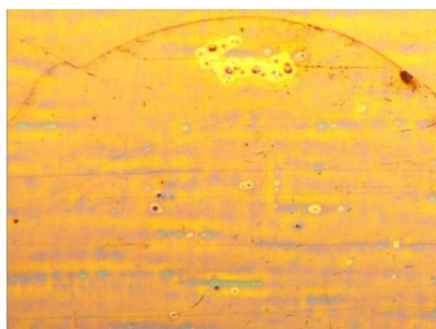

Figure 8. Microscope image of the surface of the full LED structure on metal after growth, showing macroscopic defects and pits

We demonstrated GaN/InGaN LEDs on a polycrystalline metal substrate with epitaxial GaN layers grown directly on a metal foil. LEDs on metal and sapphire showed relatively similar peak wavelength and FWHM trends with current density. LEDs on metal show 30% of the relative EQE of LEDs on sapphire, with 2.5X more TDD on metal compared to sapphire, and significantly higher leakage currents for LEDs on metal compared to LEDs on sapphire. The results presented here are preliminary, and the quality of GaN on metal can be further improved to enable higher EQE and potentially similar EQEs to LEDs on sapphire. Fabricating LEDs on metal is a new technology that can be improved in the future, with promising advantages for applications such as large-area and low-cost continuous lighting sources and displays.

6. Acknowledgements

The information, data, and work presented herein were funded in part by the Advanced Research Projects Agency – Energy (ARPA-E), U.S. Department of Energy under the SWITCHES program directed by Drs. Timothy Heidel and Isik Kizilyalli, under Award No. DE-AR0000447. We are extremely grateful to Dr. Daniel Koleske at Sandia National Laboratory for the deposition of GaN and LED layers on the metal foils by MOCVD. This work was also performed in part at the Center for Integrated Nanotechnologies, an Office of Science User Facility operated for the U.S. Department of Energy (DOE) Office of Science by Los Alamos National Laboratory (Contract 89233218CNA000001) and Sandia National Laboratories (Contract DE-NA-0003525). iBeam Materials is thankful to Chris Yung for his significant contributions to this project in the past. This paper describes objective technical results and analysis. Any subjective views or opinions that might be expressed in the paper do not necessarily represent the views of the U.S. Department of Energy or the United States Government.

7. References

[1] D. Feezell, and S. Nakamura, *Comptes Rendus Physique* **19**, 113–133 (2018).
[2] B. J. Baliga, *Semicond. Sci. Technol.* **28**, 074011 (2013).
[3] B. J. May, A. T. M. G. Sarwar, and R. C. Myers, *Appl. Phys. Lett.* **108**, 141103 (2016).
[4] J. W. Shon, J. Ohta, K. Ueno, A. Kobayashi, and H. Fujioka, *Scientific Reports* **4**, 5325 (2014).
[5] H. Kim, J. Ohta, K. Ueno, A. Kobayashi, M. Morita, Y. Tokumoto, and H. Fujioka, *Sci Rep* **7**, 1–5 (2017).
[6] J. H. Choi, A. Zoulkarneev, S. I. Kim, C. W. Baik, M. H. Yang, S. S. Park, H. Suh, U. J. Kim, H. B. Son, J. S. Lee, M. Kim, J. M. Kim, and K. Kim, *Nature Photon* **5**, 763–769 (2011).
[7] J. Kim, C. Bayram, H. Park, C.-W. Cheng, C. Dimitrakopoulos, J. A. Ott, K. B. Reuter, S. W. Bedell, and D. K. Sadana, *Nat Commun* **5**, 1–7 (2014).
[8] G. Calabrese, P. Corfdir, G. Gao, C. Pfüller, A. Trampert, O. Brandt, L. Geelhaar, and S. Fernández-Garrido, *Appl. Phys. Lett.* **108**, 202101 (2016).
[9] B. Janjua, H. Sun, C. Zhao, D. H. Anjum, D. Priante, A. A. Alhamoud, F. Wu, X. Li, A. M. Albadri, A. Y. Alyamani, M. M. El-Desouki, T. K. Ng, and B. S. Ooi, *Opt. Express, OE* **25**, 1381–1390 (2017).
[10] Y. Wu, Y. Wang, K. Sun, and Z. Mi, *Journal of Crystal Growth* **507**, 65–69 (2019).
[11] H. Sun, and X. Li, *Physica Status Solidi (a)* **216**, 1800420 (2019).
[12] H. Sun, M. K. Shakfa, M. M. Muhammed, B. Janjua, K.-H. Li, R. Lin, T. K. Ng, I. S. Roqan, B. S. Ooi, and X. Li, *ACS Photonics* **5**, 964–970 (2018).
[13] V. Matias, and C. Yung, US Patent No. 9,735,318 (15 August 2017).
[14] C. Sheehan, Y. Jung, T. Holesinger, D. M. Feldmann, C. Edney, J. F. Ihlefeld, P. G. Clem, and V. Matias, *Appl. Phys. Lett.* **98**, 071907 (2011).